

Probing the power of an electronic Maxwell Demon

Gernot Schaller,* Clive Emary, Gerold Kiesslich, and Tobias Brandes

Institut für Theoretische Physik, Technische Universität Berlin, Hardenbergstr. 36, 10623 Berlin, Germany

We suggest that a single-electron transistor continuously monitored by a quantum point contact may function as Maxwell's demon when closed-loop feedback operations are applied as time-dependent modifications of the tunneling rates across its junctions. The device may induce a current across the single-electron transistor even when no bias voltage or thermal gradient is applied. For different feedback schemes, we derive effective master equations and compare the induced feedback current and its fluctuations as well as the generated power. Provided that tunneling rates can be modified without changing the transistor level, the device may be implemented with current technology.

Maxwell's demon – a hypothetical intelligence in a box capable of sorting hot (fast) and cold (slow) atoms to left and right sub-cavities simply by matchingly inserting and removing an impenetrable wall – was initially suggested by J. C. Maxwell to highlight that thermodynamics is a macroscopic theory. Under ideal conditions, inserting and removing the wall would not require work and the apparent contradiction with the second law – the entropy in the box would be reduced and after the sorting process, work could be extracted from the temperature difference between the sub-cavities – has been a source of much debate ever since¹. It is now generally believed that this paradox is overcome by the Landauer principle²: Deleting the data required for the processing in the demon's mind would at least generate entropy $S = k_B \ln 2$ or dissipate heat of at least $Q = k_B T \ln 2$ per bit of information, yielding a net production of entropy.

The demon performs a measurement on the system (is the atom slow or fast) and conditioned on the measurement result it performs an action (opening or closing the wall), which is formally nothing but a closed-loop feedback control scheme. In our proposal, we replace the two sub-cavities of the box by two conductors that we assume to be in separate thermal equilibria. The conductors are coupled by a single resonant level, which does not require charging and spin³ effects. Conditioned on its occupation dynamics – provided by a nearby quantum point contact (QPC) – the tunneling rates to the conductors are modified in time. The feedback schemes we consider here are illustrated in Fig. 1. We will address the power production, current and statistical properties of the device.

I. METHOD

A single-electron transistor (SET) coupled to two leads in thermal equilibria may in sequential tunneling (weak coupling) approximation be well described by a Markovian Lindblad-type master equation $\dot{\rho}(t) = \mathcal{L}\rho(t)$, where – when written as a vector – $\rho(t) = (\rho_0(t), \rho_1(t))$ describes the SET part with occupation probability $\rho_1(t)$. The Liouvillian \mathcal{L} can be derived from microscopic cal-

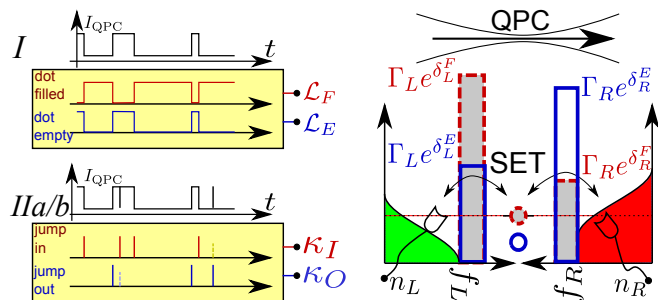


FIG. 1: (Color Online) Sketch of the setup: An SET with two attached leads (sketched are their Fermi functions f_L and f_R) is capacitively coupled to a nearby QPC. Its current I_{QPC} yields information on the instantaneous occupation of the SET. One may either apply Liouvillians \mathcal{L}_E and \mathcal{L}_F with different tunneling rates conditioned on the *present state of the SET* (scheme I, compare different tunneling barriers in SET sketch) or control operations κ_I and κ_O conditioned on the *change of the SET state* (schemes IIa/b, not shown in SET sketch). During the control operations, electrons may also tunnel into or out of the SET (dashed shorter spikes), which may not (IIa) or may (IIb) recursively trigger further control operations.

culations or simply using Fermi's golden rule and reads⁴

$$\mathcal{L} = \sum_{\alpha \in \{L, R\}} \Gamma_{\alpha} \begin{pmatrix} -f_{\alpha} & +(1-f_{\alpha}) \\ +f_{\alpha} & -(1-f_{\alpha}) \end{pmatrix}, \quad (1)$$

where Γ_{α} denotes the tunneling rate between SET and lead α and $f_{\alpha} \equiv [e^{\beta_{\alpha}(\epsilon - \mu_{\alpha})} + 1]^{-1}$ the Fermi function of lead α with corresponding inverse temperature β_{α} and chemical potential μ_{α} at the SET level ϵ (assumed to be constant throughout). Since the total number of electrons is conserved in the tunneling processes, it is possible to uniquely identify matrix elements of the Liouvillian with electronic jump processes into and out of the left and right leads, which enables one to convert Eq. (1) into an infinite set of coupled equations for (n_L, n_R) -resolved density matrices $\rho^{(n_L, n_R)}(t)$. These are conditioned on the number of electrons that have tunneled after time t into or out of the left (n_L) and right (n_R) leads. Fourier-transformation, $\rho(\chi_L, \chi_R) = \sum_{n_L, n_R} \rho^{(n_L, n_R)}(t) e^{i\chi_L n_L} e^{i\chi_R n_R}$, yields the

compact equation $\dot{\rho}(\chi_L, \chi_R, t) = \mathcal{L}(\chi_L, \chi_R)\rho(\chi_L, \chi_R, t)$ with

$$\begin{aligned} \mathcal{L}(\chi_L, \chi_R) &= \sum_{\alpha \in \{L, R\}} \Gamma_\alpha \begin{pmatrix} -f_\alpha & +(1-f_\alpha)e^{+i\chi_\alpha} \\ +f_\alpha e^{-i\chi_\alpha} & -(1-f_\alpha) \end{pmatrix} \\ &\equiv \sum_{\alpha \in \{L, R\}} \Gamma_\alpha \mathcal{F}_\alpha(\chi_\alpha). \end{aligned} \quad (2)$$

In absence of feedback, the above equation yields the complete statistics of electrons (current, noise, skewness etc.) that have tunneled across the SET⁵. At small SET bias, the QPC does not resolve to which of the attached leads a tunneling process has happened. Therefore, simplest feedback operations can only be conditioned on whether the SET is empty or filled (scheme I) or whether an electron has jumped into or out of the SET (schemes IIa/b). Such control operations may easily be included in the numerical solution of Eq. (2) via an associated stochastic Schrödinger equation⁶. For analytic results however, it is more favorable to derive an effective Liouvillian under feedback (compare appendices A, C, and D), which enables one to systematically study the effects of feedback on the statistics.

In *scheme I*, we only apply two different Liouvillians – conditioned on whether the SET is empty ($\mathcal{L}_E(\chi_L, \chi_R) \equiv \sum_{\alpha \in \{L, R\}} \Gamma_\alpha e^{\delta_\alpha^E} \mathcal{F}_\alpha(\chi_\alpha)$) or filled ($\mathcal{L}_F(\chi_L, \chi_R) \equiv \sum_{\alpha \in \{L, R\}} \Gamma_\alpha e^{\delta_\alpha^F} \mathcal{F}_\alpha(\chi_\alpha)$), where the dimensionless feedback parameters $\delta_\alpha^{E/F} \in \mathbb{R}$ encode the modification of tunneling rates and $\delta_\alpha^{E/F} = 0$ recovers the situation without feedback. The effective feedback generator reads in this case

$$\begin{aligned} \mathcal{L}_{\text{fb}}^I(\chi_L, \chi_R) &= \mathcal{L}_E(\chi_L, \chi_R) \begin{pmatrix} 1 & 0 \\ 0 & 0 \end{pmatrix} \\ &+ \mathcal{L}_F(\chi_L, \chi_R) \begin{pmatrix} 0 & 0 \\ 0 & 1 \end{pmatrix}. \end{aligned} \quad (3)$$

An extremal form of this feedback scheme would be to cut the left junction as soon as the SET is filled ($\delta_L^F \rightarrow -\infty$) and to cut the right junction when it is empty ($\delta_R^E \rightarrow -\infty$), which automatically implies unidirectional transport – independent of potential or temperature gradients. This effectively implements a feedback ratchet with two teeth – compare SET tunneling barriers in Fig. 1. However, in the idealized classical limit where the electrons are localized either on the left lead, the SET, or the right lead, this ratchet does not directly perform work as its potential does not change where the electron is localized. The resulting effective Liouvillian $\mathcal{L}_{\text{fb}}^I$ cannot generally be written in the form of Eq. (1) using modified tunneling rates $\tilde{\Gamma}_\alpha > 0$ and Fermi functions $\tilde{f}_\alpha \in (0, 1)$.

In *scheme IIa*, we instantaneously modify the SET tunneling rates by δ -kicks (compare appendix B) immediately after an electron has jumped in (e^{κ_I}) or out (e^{κ_O})

of the SET, such that

$$\begin{aligned} \kappa_I(\chi_L, \chi_R) &= \sum_{\alpha \in \{L, R\}} \delta_\alpha^I \mathcal{F}_\alpha(\chi_\alpha), \\ \kappa_O(\chi_L, \chi_R) &= \sum_{\alpha \in \{L, R\}} \delta_\alpha^O \mathcal{F}_\alpha(\chi_\alpha), \end{aligned} \quad (4)$$

where $\delta_{R/L}^{I/O} \geq 0$ are dimensionless parameters roughly given by the product of pulse width and height of time-dependent SET tunneling rates (compare appendix B). The counting-field dependence arises from the simple fact that during the control operation electrons may tunnel through the junctions (in scheme IIa, these tunneling events do not trigger further control operations): In fact, for infinitely strong feedback at one junction and zero feedback at the other junction (e.g., $\delta_L^I \rightarrow \infty$ and $\delta_R^I \rightarrow 0$) one obtains immediate equilibration of the SET with the lead to which it is tunnel-coupled (e.g., $e^{\kappa_I(0,0)}\rho \rightarrow (1-f_L, f_L)$ for all ρ). These tunneling events have to be taken into account when the complete statistics is required. Using from Eq. (2) the decomposition

$$\mathcal{F}_\alpha(\chi_\alpha) \equiv \mathcal{F}_\alpha^0 + \mathcal{F}_\alpha^+ e^{+i\chi_\alpha} + \mathcal{F}_\alpha^- e^{-i\chi_\alpha}, \quad (5)$$

where \mathcal{F}_α^+ (\mathcal{F}_α^-) is responsible for jumps into (out of) contact α and \mathcal{F}_α^0 conserves the system occupation, the full effective feedback Liouvillian reads

$$\begin{aligned} \mathcal{L}_{\text{fb}}^{IIa}(\chi_L, \chi_R) &= \sum_{\alpha \in \{L, R\}} \Gamma_\alpha \mathcal{F}_\alpha^0 \\ &+ e^{\kappa_O(\chi_L, \chi_R)} \sum_{\alpha \in \{L, R\}} \Gamma_\alpha \mathcal{F}_\alpha^+ e^{+i\chi_\alpha} \\ &+ e^{\kappa_I(\chi_L, \chi_R)} \sum_{\alpha \in \{L, R\}} \Gamma_\alpha \mathcal{F}_\alpha^- e^{-i\chi_\alpha}, \end{aligned} \quad (6)$$

such that jumps in and out of the system are immediately followed by the respective control operation. In contrast to feedback schemes modifying the system Hamiltonian^{7,8} it is no longer possible to simply shift counting fields by control operators.

For an infinitely fast QPC sampling rate, it would also be possible to recursively trigger further control operations when tunneling events take place during control. In *scheme IIb* we restrict ourselves to the case that during the control operations only one junction admits tunneling at a time, i.e., $\delta_L^I = \delta_R^O = 0$. Then, we may also derive an effective feedback master equation for a recursive feedback scheme, where electrons tunneling during a control operation would induce further control operations – possibly ad infinitum (at infinite bias and infinite feedback strength). In this case, the control operations only depend on a single counting field and we may use the decompositions (see appendix D) $e^{\kappa_O(\chi_L, \chi_R)} \equiv \mathcal{P}^O(\chi_L) = \mathcal{P}_N^O + \mathcal{P}_O^O e^{+i\chi_L} + \mathcal{P}_I^O e^{-i\chi_L}$ and $e^{\kappa_I(\chi_L, \chi_R)} \equiv \mathcal{P}^I(\chi_R) = \mathcal{P}_N^I + \mathcal{P}_I^I e^{-i\chi_R} + \mathcal{P}_O^I e^{+i\chi_R}$ together with the evident relations $\mathcal{P}_O^O(\mathcal{F}_L^+ + \mathcal{F}_R^+) = \mathcal{P}_I^I(\mathcal{F}_L^- + \mathcal{F}_R^-) = \mathcal{P}_O^O \mathcal{P}_O^I = \mathcal{P}_I^I \mathcal{P}_I^O = \mathbf{0}$ (these effectively

imply that during the control operations, the transport is unidirectional) to sum up the infinitely many terms as a von Neumann operator series. Eventually (see appendix D), this results in the effective feedback Liouvillian

$$\begin{aligned} \mathcal{L}_{\text{fb}}^{Ib}(\chi_L, \chi_R) = & \sum_{\alpha \in \{L, R\}} \Gamma_{\alpha} \mathcal{F}_{\alpha}^0 \\ & + (\mathcal{P}_N^O + e^{-i\chi_L} \mathcal{P}_N^I \mathcal{P}_I^O) \times \\ & \times \left[\mathbf{1} - \mathcal{P}_O^I \mathcal{P}_I^O e^{i(\chi_R - \chi_L)} \right]^{-1} \times \\ & \times \left(\sum_{\alpha \in \{L, R\}} \Gamma_{\alpha} \mathcal{F}_{\alpha}^+ e^{+i\chi_{\alpha}} \right) \\ & + (\mathcal{P}_N^I + e^{+i\chi_R} \mathcal{P}_N^O \mathcal{P}_O^I) \times \\ & \times \left[\mathbf{1} - \mathcal{P}_I^O \mathcal{P}_O^I e^{i(\chi_R - \chi_L)} \right]^{-1} \times \\ & \times \left(\sum_{\alpha \in \{L, R\}} \Gamma_{\alpha} \mathcal{F}_{\alpha}^- e^{-i\chi_{\alpha}} \right). \quad (7) \end{aligned}$$

Eqns. (3), (6), (7) yield the complete statistics for the current through the SET under the different feedback schemes: The generating function for its cumulants is in the long term given by the dominant (with $\lambda(0, 0) = 0$) eigenvalue $\lambda(\chi_L, \chi_R)$ of the effective Liouvillians. We have checked numerically (see appendixes A, C, and D) that the analytic results from the effective master equation coincide for all schemes with an ensemble-average of the stochastic Schrödinger equation with feedback explicitly included. In the idealized classical limit, none of the schemes performs work on the system. However, quantum-mechanically the time-dependent modification of the tunneling rates changes the energy spectrum of the total Hamiltonian and thereby performs work⁹.

II. CURRENT AND FLUCTUATIONS

We summarize the behavior of the current for finite feedback strengths at reverse infinite bias ($f_L = 0$, $f_R = 1$), zero bias ($f_L = f_R = f$), and infinite bias ($f_L = 1$, $f_R = 0$) for the different feedback schemes in table I. For finite temperatures (where $0 < f < 1$) feed-

scheme	$V_{\text{bias}} \rightarrow -\infty$	$V_{\text{bias}} = 0$	$V_{\text{bias}} \rightarrow +\infty$
I	$-e^{-\delta_{\text{fb}}}/2$	$2f(1-f) \sinh(\delta_{\text{fb}})$	$e^{\delta_{\text{fb}}}/2$
IIa	$-1/2$	$f(1-f)(1 - e^{-\delta_{\text{fb}}})$	$1 - e^{-\delta_{\text{fb}}}/2$
IIb	$-1/2$	$\frac{f(1-f)(e^{\delta_{\text{fb}}}-1)}{2f(1-f)+e^{\delta_{\text{fb}}}[1-2f(1-f)]}$	$e^{\delta_{\text{fb}}}/2$

TABLE I: Values of the current (in units of $\Gamma_L = \Gamma_R = \Gamma$) under finite but symmetric feedback. The feedback parameters have been chosen as $\delta_L^F = \delta_R^E = -\delta_{\text{fb}}$ and $\delta_R^F = \delta_L^E = \delta_{\text{fb}}$ for scheme I and $\delta_R^I = \delta_L^O = \delta_{\text{fb}}$ as well as $\delta_L^I = \delta_R^O = 0$ for schemes IIa and IIb, respectively.

back may induce a current even at zero bias, such that the

device acts as a demon shuffling electrons from one bath to another (here from left to right) using only information on SET occupancy. This has to be contrasted with feedback ratchets¹⁰ where the time-dependent ratchet potential performs work. The apparent divergence of the current in feedback scheme I for infinite bias and feedback strength is natural as the tunneling rates diverge likewise. For feedback scheme IIb however, we observe a genuine feedback catastrophe for large bias and large feedback strength leading to a divergent current: Control operations mutually trigger further control operations with vanishing halting probability, which leads to avalanche-like transport. Therefore, in contrast to scheme I, the Fano factor $F = S/|I|$ given by the ratio of noise and current – as summarized in Table II – also diverges in this region when we let the feedback strength go to infinity.

scheme	$V_{\text{bias}} = 0$	$V_{\text{bias}} \rightarrow +\infty$
I	$\coth(\delta_{\text{fb}})/2 + (1-2f)^2 \tanh(\delta_{\text{fb}})/2$	$1/2$
IIa	$\frac{2f(1-f) + \cosh(\delta_{\text{fb}})[1-2f(1-f)] + \sinh(\delta_{\text{fb}})}{(1-2f)^2 [\cosh(\delta_{\text{fb}}) - 1] + \sinh(\delta_{\text{fb}})}$	$\frac{4-3e^{-\delta_{\text{fb}}}}{4-2e^{-\delta_{\text{fb}}}}$
IIb	$\frac{2e^{2\delta_{\text{fb}}} - e^{\delta_{\text{fb}}} + 1}{e^{2\delta_{\text{fb}}} - 1}$	$e^{\delta_{\text{fb}}} - 1/2$

TABLE II: Values of the Fano factor (assuming $\delta_{\text{fb}} \geq 0$) for zero and infinite bias with the same parameters as in table I, the zero-bias Fano factor for scheme IIb has been evaluated for $f = 1/2$ only for brevity. The reverse infinite bias Fano factor (not shown) is $1/2$ for all schemes independent of feedback. Divergence of the infinite bias Fano factor for scheme IIb at infinite feedback strength $\delta_{\text{fb}} \rightarrow \infty$ demonstrates the feedback catastrophe. Also, at zero feedback the Fano factor should diverge at zero bias as this is the point where conventionally the current would vanish.

Naturally, there exists a parameter regime where the device transports electrons against an existing electrical or thermal gradient, where e.g., electrons are transported from left to right even though $f_L < f_R$, compare also Fig. 2. For scheme I, this effectively implements a Parrondo game (ratchet): Playing two losing strategies (tunneling with the bias) in an alternating manner may yield a winning strategy (tunneling against the bias)¹¹. For our model, feedback is necessary to achieve such a current inversion: Without feedback, the long-term cumulant-generating function for the current obeys the analytic relation $\lambda(0, -\chi) = \lambda\left(0, +\chi - i \ln \left[\frac{(1-f_L)f_R}{f_L(1-f_R)} \right] \right)$, which when both leads are at the same temperature eventually leads to the fluctuation theorem¹²⁻¹⁴ $\lim_{t \rightarrow \infty} \frac{P_n(t)}{P_{-n}(t)} = e^{+n\beta(\mu_L - \mu_R)}$. This implies that for a constant Liouvillian (1), the current $I = \lim_{t \rightarrow \infty} d/dt \sum_n n P_n(t)$ always flows from reservoirs with large chemical potential towards the reservoir with the smaller chemical potential. Also with open-loop feedback, where control operations are applied unconditionally (e.g., in a random or periodic manner), we find that the current will never flow against the electro-thermal gradient – as long as no work is performed on the SET itself (i.e., the SET level ϵ remains

unchanged), see appendix E.

For scheme I we find that the Johnson-Nyquist relation normally relating noise with differential conductance at zero bias voltage (at similar temperatures left and right) is now shifted to the equilibrium voltage $V^* = (-\delta_L^E - \delta_R^F + \delta_R^E + \delta_L^F) / \beta$ at which the current vanishes $I(V^*) = 0$, i.e., more explicitly we have $S|_{V=V^*} = \frac{2}{\beta} \frac{dI}{dV}|_{V=V^*}$. We obtain a similarly simple modification of the fluctuation theorem for the electron counting statistics under feedback: The cumulant-generating function for the current obeys

$$\lambda^I(-\chi) = \lambda^I \left(+\chi - i \ln \left[\frac{(1-f_L)f_R}{f_L(1-f_R)} e^{\beta V^*} \right] \right), \quad (8)$$

which for both leads at the same temperature yields for the counting statistics $\lim_{t \rightarrow \infty} \frac{P_n(t)}{P_{-n}(t)} = e^{n\beta(\mu_L - \mu_R - V^*)}$.

This formula directly demonstrates that the current may be directed against a potential gradient when the feedback parameters and hence V^* are adjusted accordingly.

For feedback schemes IIa and IIb, the equilibrium voltage V^* can be obtained numerically and depends on the baseline tunneling rates Γ_α .

III. MAXIMUM POWER AT MAXIMUM FEEDBACK

For schemes IIa and IIb we may take $\delta_R^I = \delta_L^O \rightarrow \infty$ and $\delta_L^I = \delta_R^O = 0$ to obtain the maximum effect, but to bound the Liouvillian for scheme I we constrain ourselves to finite feedback strengths $\delta_L^E = \delta_R^F = +\delta_{fb}$ and $\delta_R^E = \delta_L^F = -\delta_{fb}$. The power $P = -IV$ generated by the demon can – when both leads are at the same temperature β be evaluated as $P\beta = -I\beta(\mu_L - \mu_R) = -I(f_L, f_R) \ln \left[\frac{f_L(1-f_R)}{f_R(1-f_L)} \right]$. The right hand side of this expression can for given Γ_L and Γ_R be numerically maximized with respect to the Fermi functions $f_{L/R} \in (0, 1)$ yielding the maximum power generated by the device, see table III. The maximum power generated with scheme I

scheme	$\Gamma_L = \Gamma_R = \Gamma$	$\Gamma_{\max} \gg \Gamma_{\min}$
IIa	$0.0841 \Gamma k_B T$	$0.1219 \Gamma_{\max} k_B T$
IIb	$0.1892 \Gamma k_B T$	$0.1589 \Gamma_{\max} k_B T$

TABLE III: Maximum power generated with the device for schemes IIa and IIb at maximum unidirectional feedback for symmetric and highly asymmetric tunneling rates.

is unbounded (as the Liouvillian) and asymptotically approaches $0.2785 \Gamma e^{\delta_{fb}} k_B T$ for symmetric tunneling rates. Even under idealized conditions, the associated work performed by the demon has to be contrasted with the heat dissipated when the QPC trajectory's data-points are deleted (Landauer principle). To perform the continuous monitoring of the SET it is important that the QPC sampling rate $\Delta\tau^{-1}$ is greater than the maximum tunneling rate $\Delta\tau < \Gamma_{\max}^{-1}$ (or $\Delta t \leq \Gamma_{\max} e^{-\delta_{fb}}$ for scheme I).

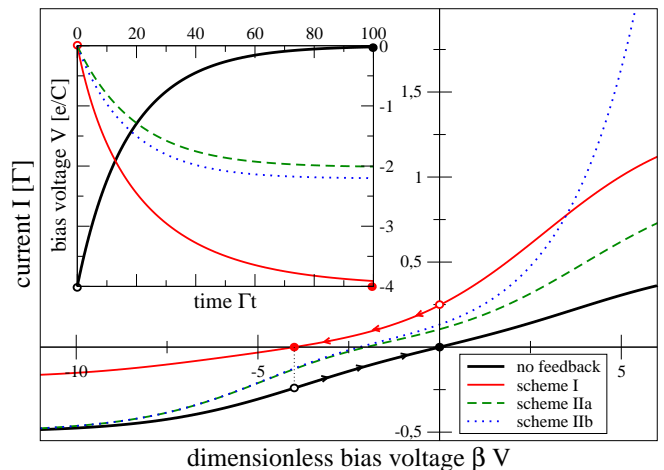


FIG. 2: (Color Online) Current-voltage characteristics under feedback strength $\delta_L^E = \delta_R^F = -\delta_R^E = -\delta_L^F = 1$ in scheme I (thin solid curve, red), maximum feedback in schemes IIa and IIb (dashed and dotted, respectively) and no feedback (bold black) for symmetric tunneling rates $\Gamma_L = \Gamma = \Gamma_R$ and $\beta\epsilon = 2$. The current may point in the other direction than the voltage leading to a positive power generated by the device. The inset (for $\beta e/C = 1$) shows the mean-field evolution of the voltage from an initial value (empty circles) to the stable fixed points (filled circle) for symmetric capacitances of the two conductors.

This implies that the maximum work per current measurement $W = P_{\max} \Delta\tau$ is always smaller than the dissipated Landauer heat $Q \geq k_B T \ln 2$ by the demon, such that the results are compatible with the second law.

IV. FEEDBACK CHARGING EFFECTS

Small leads of finite capacitances will usually be driven out of equilibrium due to transport. Additional larger reservoirs at thermal equilibrium may however immediately re-enforce equilibrium in the leads solely by scattering interactions (without electron tunneling). We may phenomenologically include this effect by making the chemical potentials dependent on the number of tunneled particles: Starting at equilibrium, the difference V in chemical potentials between the two leads is classically simply proportional to the number of tunneled particles $V = en/C$, where C denotes the total capacitance (similar relations hold for left and right chemical potentials in case of asymmetric capacitances¹⁵). We may numerically solve the resulting mean-field nonlinear (compare appendix F) differential equation $\dot{V} = e/C \langle \dot{n}(t) \rangle = eI(V)/C$ to obtain the dynamical evolution $V(t)$, compare the inset in Fig. 2. After the equilibrium voltage ($I(V^*) = 0$) has been approached, feedback may be stopped and the current will reverse its direction (black trajectory). With the QPC already in place, it appears reasonable to use it as a detector to clearly discriminate the resulting initial fluctuations from

equilibrium ones. This scheme works as an accumulator undergoing charging (feedback) and discharging (no-feedback) cycles, where the total stored energy is given by $W = C(V^*)^2/(2e)$.

V. EXPERIMENTAL IMPLEMENTATION

With gate voltages, the height of the tunneling barriers may be adjusted such that the timescale on which electrons tunnel through the QPC can be tuned from ms¹⁶ to seconds and even hours. For periodically varying gate voltages, the frequency corresponds with 100 MHz to switching times five orders of magnitude smaller in recent electron pumping experiments^{17,18}. The bandwidth of typical experimental QPC detector devices has been reported in the range of 40 kHz, with sufficiently larger current sampling frequencies of 100 kHz¹⁹. The experimental challenge therefore clearly lies in the necessity of strongly modifying the tunneling rates without performing work on the system (changing the SET level). With gate electrodes of sizes below 100 nm¹⁸ it should be possible to keep the energy level of the SET (size about 300 nm¹⁶) approximately constant.

VI. SUMMARY

To conclude, we have compared several closed-loop feedback schemes implementing Maxwell's demon by

means of an effective feedback master equation. Scheme I used a piecewise constant Liouvillian conditioned on the time-dependent SET occupation, whereas schemes IIa and IIb were conditioned on its change and used δ -kicks in the tunneling rates. All schemes are capable of generating a current against a moderate bias – which is for constant SET level not possible for open-loop schemes – and may for finite-size leads be used to charge a feedback battery. With Landauer's principle, the second law is of course respected by the device. Schemes I and IIa (with necessarily small feedback strength) should be implementable with present-day technology, whereas the feedback recursion depth appears to be currently limited by the QPC sampling frequency. Schemes with finite recursion depth are however also treatable with the methods in this article.

VII. ACKNOWLEDGEMENTS

Financial support by the DFG (grant SCHA 1646/2-1, SFB 910) and stimulating discussions with T. Novotný and M. Rinck are gratefully acknowledged.

* Electronic address: gernot.schaller@tu-berlin.de

- ¹ K. Maruyama, F. Nori, and V. Vedral, *Rev. Mod. Phys.* **81**, 1 (2009).
- ² R. Landauer, *IBM J. Res. Dev.* **5**, 183 (1961).
- ³ S. Datta, e-print arXiv:0704.1623v1.
- ⁴ M. Esposito and K. Lindenberg and C. Van den Broeck, *Europhys. Lett.* **85**, 60010 (2009).
- ⁵ Y. V. Nazarov, *Quantum Noise in Mesoscopic Physics*, Kluwer Academic, Dordrecht (2003).
- ⁶ H.-P. Breuer and F. Petruccione, *The Theory of Open Quantum Systems*, Oxford University Press (2002).
- ⁷ H. M. Wiseman and G. J. Milburn, *Quantum Measurement and Control*, Cambridge University Press (2010).
- ⁸ G. Kiesslich, G. Schaller, C. Emary, and T. Brandes, to be published by *Phys. Rev. Lett.*, e-print arXiv:1102.3771.
- ⁹ S. W. Kim, T. Sagawa, S. De Liberato, and M. Ueda, *Phys. Rev. Lett.* **106**, 070401 (2011).
- ¹⁰ F. J. Cao, M. Feito, and H. Touchette, *Physica A* **388**, 113 (2009).
- ¹¹ G. P. Harmer and D. Abbott, *Nature* **402**, 864 (1999).
- ¹² M. Esposito, U. Harbola, and S. Mukamel, *Rev. Mod. Phys.* **81**, 1665 (2009).
- ¹³ K. Saito and Y. Utsumi, *Phys. Rev. B* **78**, 115429 (2008).
- ¹⁴ Y. Utsumi and K. Saito, *Phys. Rev. B* **79**, 235311 (2009).
- ¹⁵ J. D. Jackson, *Classical Electrodynamics*, John Wiley and Sons, New York (1998).

- ¹⁶ S. Gustavsson, R. Leturcq, B. Simovic, R. Schleser, T. Ihn, P. Studerus, K. Ensslin, D. C. Driscoll and A. C. Gossard, *Phys. Rev. Lett.* **96**, 076605 (2006).
- ¹⁷ M. D. Blumenthal, B. Kaestner, L. Li, S. Giblin, T. J. B. M. Janssen, M. Pepper, D. Anderson, G. Jones, and D. A. Ritchie, *Nature Physics* **3**, 343 (2007).
- ¹⁸ N. Maire, F. Hohls, B. Kaestner, K. Pierz, H. W. Schumacher, and R. J. Haug, *Appl. Phys. Lett.* **92**, 082112 (2008).
- ¹⁹ C. Flindt, C. Fricke, F. Hohls, T. Novotny, K. Netocny, T. Brandes, and R. J. Haug, *PNAS* **106**, 10116 (2009).

Appendix A: Justification of scheme I

Assuming that the dot is empty at time t , i.e., $\rho(t) = (1, 0)$, its no-measurement time evolution under feedback scheme I will be governed by $\rho(t + \Delta t) = e^{\mathcal{L}_E(\chi_L, \chi_R)\Delta t}\rho(t)$, whereas for an initially filled dot $\rho(t) = (0, 1)$, we will have the evolution $\rho(t + \Delta t) = e^{\mathcal{L}_F(\chi_L, \chi_R)\Delta t}\rho(t)$. Using projection superoperators on the empty and filled dot states, respectively, both cases can

be incorporated into a single equation

$$\begin{aligned} \rho(t + \Delta t) = & e^{\mathcal{L}_E(\chi_L, \chi_R)\Delta t} \begin{pmatrix} 1 & 0 \\ 0 & 0 \end{pmatrix} \rho(t) \\ & + e^{\mathcal{L}_F(\chi_L, \chi_R)\Delta t} \begin{pmatrix} 0 & 0 \\ 0 & 1 \end{pmatrix} \rho(t). \quad (\text{A1}) \end{aligned}$$

Expanding the propagators for small Δt , using that the projection operators add up to the identity, and solving

Therefore, the original counting fields may be kept, and effectively, the Liouvillian (3) has the first column from \mathcal{L}_E and the second column from \mathcal{L}_F

$$\mathcal{L}_{\text{fb}}^I(\chi_L, \chi_R) = \begin{pmatrix} -\Gamma_L e^{\delta_L^E} f_L - \Gamma_R e^{\delta_R^E} f_R & +\Gamma_L e^{\delta_L^F} e^{+i\chi_L} (1 - f_L) + \Gamma_R e^{\delta_R^F} e^{+i\chi_R} (1 - f_R) \\ +\Gamma_L e^{\delta_L^E} e^{-i\chi_L} f_L + \Gamma_R e^{\delta_R^E} e^{-i\chi_R} f_R & -\Gamma_L e^{\delta_L^F} (1 - f_L) - \Gamma_R e^{\delta_R^F} (1 - f_R) \end{pmatrix}, \quad (\text{A2})$$

which explicitly breaks detailed balance.

A single trajectory for this feedback scheme may be generated as follows: Assuming that e.g., the dot is initially filled, the probability that during a small timestep Δt the electron jumps out to the left is given by $P_{\text{left}}^F(\Delta t) = \Delta t \Gamma_L e^{\delta_L^F} (1 - f_L)$, whereas the probability to jump out to the right reads $P_{\text{right}}^F(\Delta t) = \Delta t \Gamma_R e^{\delta_R^F} (1 - f_R)$. The probabilities for electrons jumping from left or right lead into an initially empty dot are obtained similarly and read $P_{\text{left}}^E(\Delta t) = \Delta t \Gamma_L e^{\delta_L^E} f_L$ and $P_{\text{right}}^E(\Delta t) = \Delta t \Gamma_R e^{\delta_R^E} f_R$. Using a random number generator, one may with sufficiently small timesteps (such that the jump probabilities are significantly smaller than one) generate single trajectories for the dot occupation n_{SET} , the number of tunneled particles to the left lead n_L , and the number of particles tunneled to the right lead n_R . The ensemble average of many such trajectories may now be compared with the analytic solution of the effective feedback master equation (3), see Fig. 3. It follows that for sufficiently many trajectories the same average observables will be obtained as with the effective feedback master equation.

Appendix B: δ -kick propagators

There are multiple derivations of delta-kick propagators, we provide a simple pedestrians derivation based on piecewise constant time dependencies as used in scheme I. When $\mathcal{L}(t)$ is a matrix that does not commute with itself at different times, the equation $\dot{\rho}(t) = \mathcal{L}(t)\rho(t)$ is impossible to solve analytically in the general case. However, when the Liouvillian $\mathcal{L}(t)$ is piecewise constant, the solution may be readily obtained by conventionally propagating for a time period where the Liouvillian is constant, and using the resulting state as an initial value for the next propagation period with another constant

for the finite-difference $[\rho(t + \Delta t) - \rho(t)]/\Delta t$ yields the effective feedback Liouvillian Eq. (3) when $\Delta t \rightarrow 0$. The switching between the different propagators is assumed to be instantaneous, such that during the switching time, no particles may tunnel.

Liouvillian.

Let us therefore assume a constant baseline Liouvillian superimposed with an additional control Liouvillian $\mathcal{L}(t) = \mathcal{L}_0 + \mathcal{L}_c \Theta(t - t_c) \Theta(t_c + \tau_c - t)$, where the latter is turned on at time t_c and lasts for timespan τ_c ($\Theta(x)$ denotes the Heaviside step function). The solution for all times reads in this case

$$\rho(t) = \begin{cases} e^{\mathcal{L}_0 t} \rho_0 & : t \leq t_c \\ e^{(\mathcal{L}_0 + \mathcal{L}_c)(t - t_c)} e^{\mathcal{L}_0 t_c} \rho_0 & : t_c < t < t_c + \tau_c \\ e^{\mathcal{L}_0(t - t_c - \tau_c)} e^{(\mathcal{L}_0 + \mathcal{L}_c)\tau_c} e^{\mathcal{L}_0 t_c} \rho_0 & : t_c + \tau_c \leq t \end{cases}.$$

We now assume that the control Liouvillian scales inversely with the pulse duration $\mathcal{L}_c = \frac{\kappa_c}{\tau_c}$ with κ_c being a dimensionless super-operator of Lindblad form. Letting the pulse duration vanish $\tau_c \rightarrow 0$, we approximate a δ -kick via $\mathcal{L}(t) = \mathcal{L}_0 + \kappa_c \delta(t - t_c)$ (where $\delta(x)$ represents the Dirac- δ distribution), such that the solution reads

$$\rho(t) = \begin{cases} e^{\mathcal{L}_0 t} \rho_0 & : t \leq t_c \\ e^{\mathcal{L}_0(t - t_c)} e^{\kappa_c} e^{\mathcal{L}_0 t_c} \rho_0 & : t_c \leq t \end{cases}, \quad (\text{B1})$$

that is, the constant propagator evolution is simply interrupted by the control operation e^{κ_c} at control time t_c .

Experimentally, it may be more reasonable to discuss smooth dependencies $\mathcal{L}(t) = \mathcal{L}_0 + \mathcal{L}_c(t - t_c)$ with the assumptions $\mathcal{L}_c(x < -\tau_c/2) = \mathcal{L}_c(x > +\tau_c/2) = \mathbf{0}$ and that $\int \mathcal{L}_c(t) dt$ is independent of the pulse duration τ_c . The latter condition also implies that the maximum pulse height must scale inversely with the pulse duration. In the limit of vanishing pulse duration $\tau_c \rightarrow 0$ such a control operation would also converge to a Dirac- δ distribution, such that during control, the baseline Liouvillian \mathcal{L}_0 may be neglected and we would have an effective propa-

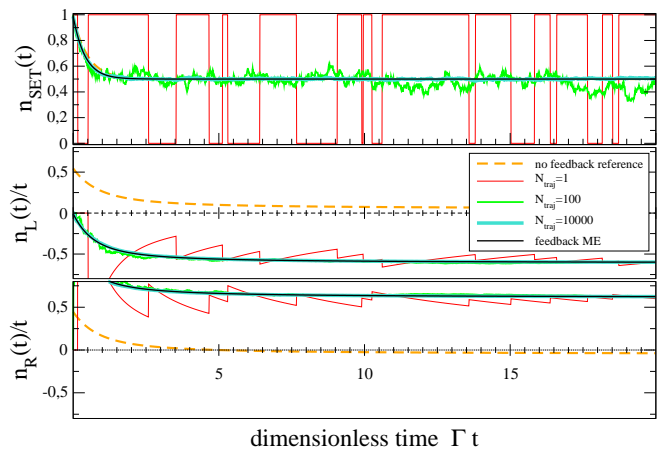


FIG. 3: (Color Online) Comparison of a single (thin red curve with jumps, same realization in all panels) and the average of 100 (medium thickness, green) and 10000 (bold smooth curve, turquoise) trajectories with the solution from the effective feedback master equation [Eq. (3), thin black] for the dot occupation (top), the number of particles on the left (middle), and the number of particles on the right (bottom). The average of the trajectories converges to the effective feedback master equation result. The reference curve without feedback (dashed orange) may be obtained from Eq. (2) or by using vanishing feedback parameters and demonstrates that the direction of the current may actually be reversed via sufficiently strong feedback. Parameters: $\Gamma_L = \Gamma_R \equiv \Gamma$, $f_L = 0.45$, $f_R = 0.55$, $\delta_L^E = \delta_R^E = 1.0$, $\delta_R^E = \delta_L^E = -10.0$, and $\Gamma\Delta t = 0.01$.

gator

$$\kappa_c \equiv \lim_{\tau_c \rightarrow 0} \int_{-\tau_c/2}^{+\tau_c/2} \mathcal{L}_c(t') dt', \quad (\text{B2})$$

which must be dimensionless and inherits the Lindblad form from $\mathcal{L}_c(t)$.

Appendix C: Justification of scheme IIa

When ultrashort (in the sense discussed in Appendix B) control operations on the SET tunneling rates are only to be applied immediately after an electron jumps into or out of the dot, the derivation of an effective master equation is a bit more involved. We start from the inverse Fourier transform of the evolution generated by Eq. (2)

$$\begin{aligned} \rho^{(n_L, n_R)}(t + \Delta t) &= \mathcal{J}^{(n_L, n_R)}(\Delta t) \rho(t), \\ \mathcal{J}^{(n_L, n_R)}(\Delta t) &\equiv \int_{-\pi}^{+\pi} \frac{d^2 \chi_\alpha}{4\pi^2} e^{\mathcal{L}(\chi_L, \chi_R) \Delta t - in_L \cdot \chi_L - in_R \cdot \chi_R}, \end{aligned} \quad (\text{C1})$$

where $\rho(t)$ denotes the unconditional dot density matrix at time t , and $n_{L/R}$ the number of electrons that have tunneled to left/right reservoirs during the timestep Δt . For small Δt it suffices to consider single-particle jumps only. Expanding the propagator for small Δt and using the orthonormality relation $\int_{-\pi}^{+\pi} e^{i(n-m)\chi} d\chi = 2\pi\delta_{nm}$ we obtain the conditional evolution equations

$$\begin{aligned} \rho^{(0,0)}(t + \Delta t) &= [\mathbf{1} + \Delta t (\Gamma_L \mathcal{F}_L^0 + \Gamma_R \mathcal{F}_R^0)] \rho(t), \\ \rho^{(+1,0)}(t + \Delta t) &= \Gamma_L \Delta t \mathcal{F}_L^+ \rho(t), \\ \rho^{(-1,0)}(t + \Delta t) &= \Gamma_L \Delta t \mathcal{F}_L^- \rho(t), \\ \rho^{(0,+1)}(t + \Delta t) &= \Gamma_R \Delta t \mathcal{F}_R^+ \rho(t), \\ \rho^{(0,-1)}(t + \Delta t) &= \Gamma_R \Delta t \mathcal{F}_R^- \rho(t), \end{aligned} \quad (\text{C2})$$

and the respective probabilities are given by the trace of these operators. To derive a master equation accounting for the average evolution of observables without feedback one may simply compute the weighted average $\bar{\rho}(t + \Delta t) = \rho^{(0,0)} + \rho^{(+1,0)} + \rho^{(-1,0)} + \rho^{(0,+1)} + \rho^{(0,-1)}$, which would after solving for the finite difference scheme $(\bar{\rho}(t + \Delta t) - \rho(t))/\Delta t$ yield the original Liouvillian in Eq. (1) when $\Delta t \rightarrow 0$. In contrast, with δ -kick feedback operations (compare appendix B) e.g.

$$\begin{aligned} \kappa_I &= \int_{-\tau_c/2}^{+\tau/2} \mathcal{L}_I^{\text{control}}(t') dt' \\ &= \delta_L^I \mathcal{F}_L(0) + \delta_R^I \mathcal{F}_R(0), \end{aligned} \quad (\text{C3})$$

compare Eq. (2) and similarly for κ_O , where $\delta_\alpha^{I/O} \equiv \int_{-\tau_c/2}^{+\tau/2} \Gamma_\alpha^{I/O}(t) dt'$ are dimensionless feedback parameters (characterizing the product of height and width of the time-dependent control tunneling rates $\Gamma_\alpha^{I/O}(t)$), we have to perform the average after applying the matching feedback operation [in (I) or out (O)]

$$\begin{aligned} \bar{\rho}(t + \Delta t) &= \rho^{(0,0)} + e^{\kappa_O} \rho^{(+1,0)} + e^{\kappa_I} \rho^{(-1,0)} \\ &\quad + e^{\kappa_O} \rho^{(0,+1)} + e^{\kappa_I} \rho^{(0,-1)}. \end{aligned} \quad (\text{C4})$$

After converting this into a finite-difference equation we would obtain the generator in Eq. (6) without counting fields. Now it is essential that during the control operations, electrons may tunnel through the junctions: Although the pulse duration is infinitesimally small, the product of pulse height and pulse width remains constant, such that the tunneling probability is characterized by the feedback strength. Therefore, counting fields may be re-introduced via a conditional master equation as was done when deriving Eq. (2) from Eq. (1). Finally, this yields the form of Eq. (6).

For the trajectories we constrain ourselves to opening only one junction at a time for all control operations, e.g., $\delta_L^I = \delta_R^O = 0$ in order to avoid an unbounded number of particles tunneling during control. It is straightforward

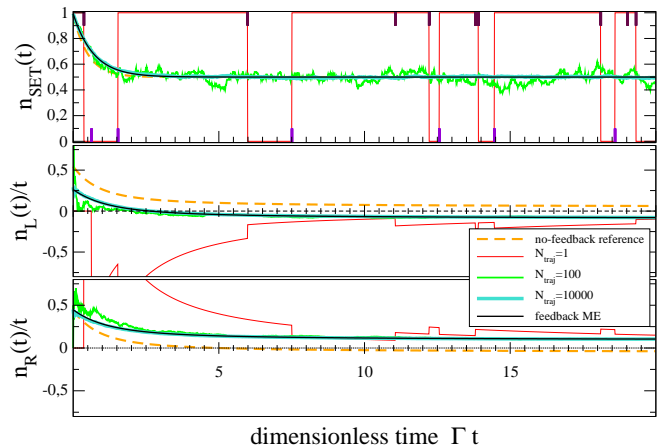


FIG. 4: (Color Online) Comparison of a single and the average of 100 and 10000 trajectories with the solution from the effective feedback master equation (6) for the dot occupation (top), the number of particles on the left (middle), and the number of particles on the right (bottom). The average of the trajectories converges to the effective feedback master equation result. The single trajectory only records the state after all control operations have been performed, i.e., jumps with no net effect are not visible. Therefore, control operations (bold kinks in top graph) are not always correlated with a net change in the occupation or the particle number left and right. The second last top kink for example stands for a out-control operation e^{κ_O} that was triggered by an electron jumping to the left (an information which is not provided by the QPC) contact. During the control operation, an electron jumped back from the left contact to the system, such that no net change in n_{dot} , n_L , nor n_R occurred. Color coding and parameters are as in Fig. 3 where applicable. Feedback parameters were chosen as $\delta_L^I = \delta_R^O = 0$ and $\delta_R^I = \delta_L^O = 1.0$.

to compute the trajectories as described in appendix A, see Fig. 4. The computed trajectories do well converge to the results of the effective feedback master equation. The scheme is non-recursive, i.e., electrons tunneling during control operations do not trigger a further control operation.

Appendix D: Justification of scheme IIb

In order to resum the control operations when applied recursively, it is essential that only one junction is opened at a time, formally expressed by choosing $\delta_L^I = \delta_R^O = 0$. This implies that once a control operation has been triggered initially, the transport becomes unidirectional, which allows for a simple analytic resummation.

We note that in this case the control operations only depend on a single counting field and we have in their matrix exponential the simple decomposition

$$e^{\kappa_O(\chi_L, \chi_R)} \equiv \mathcal{P}^O(\chi_L) \equiv \mathcal{P}_N^O + \mathcal{P}_O^O e^{+i\chi_L} + \mathcal{P}_I^O e^{-i\chi_L} = \begin{pmatrix} 1 - (1 - e^{-\delta_L^O})f_L & e^{+i\chi_L}(1 - e^{-\delta_L^O})(1 - f_L) \\ e^{-i\chi_L}(1 - e^{-\delta_L^O})f_L & 1 - (1 - e^{-\delta_L^O})(1 - f_L) \end{pmatrix},$$

$$e^{\kappa_I(\chi_L, \chi_R)} \equiv \mathcal{P}^I(\chi_R) \equiv \mathcal{P}_N^I + \mathcal{P}_O^I e^{+i\chi_R} + \mathcal{P}_I^I e^{-i\chi_R} = \begin{pmatrix} 1 - (1 - e^{-\delta_R^I})f_R & e^{+i\chi_R}(1 - e^{-\delta_R^I})(1 - f_R) \\ e^{-i\chi_R}(1 - e^{-\delta_R^I})f_R & 1 - (1 - e^{-\delta_R^I})(1 - f_R) \end{pmatrix}, \quad (\text{D1})$$

where the upper index labels the trigger process and the lower indices mark the parts responsible for no particle change (N), a particle jumping out of the system (O, possible for κ_I only to the right), and a particle jumping into the system (I, possible for κ_O only from the left).

The fact that out of an empty system, no particle may jump out and vice versa for a filled SET system no further particle may jump in is formally reflected in the relations $\mathcal{P}_O^O \mathcal{F}_B^+ = \mathcal{P}_O^O \mathcal{F}_L^+ = \mathbf{0}$ and $\mathcal{P}_I^I \mathcal{F}_L^- = \mathcal{P}_I^I \mathcal{F}_R^- = \mathbf{0}$ as well as $\mathcal{P}_I^I \mathcal{P}_I^O = \mathcal{P}_O^O \mathcal{P}_O^I = \mathbf{0}$. Therefore, the first-order feedback master equation for scheme IIa in Eq. (6) reduces in this

case ($\delta_L^I = \delta_R^O = 0$) to

$$\mathcal{L}_{\text{fb}}^{(1)} = \Gamma_L \mathcal{F}_L^0 + \Gamma_R \mathcal{F}_R^0 + (\mathcal{P}_N^O + \mathcal{P}_I^O e^{-i\chi_L})(\Gamma_L e^{+i\chi_L} \mathcal{F}_L^+ + \Gamma_R e^{+i\chi_R} \mathcal{F}_R^+) + (\mathcal{P}_N^I + \mathcal{P}_O^I e^{+i\chi_R})(\Gamma_L e^{-i\chi_L} \mathcal{F}_L^- + \Gamma_R e^{-i\chi_R} \mathcal{F}_R^-). \quad (\text{D2})$$

To generalize this scheme to recursive feedback scheme (IIb) with a potentially infinite recursion depth requires to recursively follow the scheme $\mathcal{L}_{\text{fb}}^{(i)} \rightarrow \mathcal{L}_{\text{fb}}^{(i+1)}$ by performing in each iteration the replacements

$$\begin{aligned} \mathcal{P}_N^O \mathcal{A} &\rightarrow \mathcal{P}_N^O \mathcal{A}, \\ \mathcal{P}_I^O \mathcal{A} &\rightarrow (\mathcal{P}_N^I + \mathcal{P}_O^I e^{+i\chi_R}) \mathcal{P}_I^O \mathcal{A}, \\ \mathcal{P}_N^I \mathcal{A} &\rightarrow \mathcal{P}_N^I \mathcal{A}, \\ \mathcal{P}_O^I \mathcal{A} &\rightarrow (\mathcal{P}_N^O + \mathcal{P}_I^O e^{-i\chi_L}) \mathcal{P}_O^I \mathcal{A} \end{aligned} \quad (\text{D3})$$

for arbitrary operators \mathcal{A} (in this recipe we have also used that $\mathcal{P}_I^I \mathcal{P}_I^O = \mathcal{P}_O^O \mathcal{P}_O^I = \mathbf{0}$), which eventually leads to

$$\begin{aligned} \mathcal{L}_{\text{fb}}^{(\infty)} &= \Gamma_L \mathcal{F}_L^0 + \Gamma_R \mathcal{F}_R^0 \\ &+ (\mathcal{P}_N^O + \mathcal{P}_N^I \mathcal{P}_O^I e^{-i\chi_L}) \times \\ &\times \left[\sum_{n=0}^{\infty} (\mathcal{P}_I^O \mathcal{P}_I^O)^n e^{+in(\chi_R - \chi_L)} \right] \times \\ &\times (\Gamma_L e^{+i\chi_L} \mathcal{F}_L^+ + \Gamma_R e^{+i\chi_R} \mathcal{F}_R^+) \\ &+ (\mathcal{P}_N^I + \mathcal{P}_N^O \mathcal{P}_O^I e^{+i\chi_R}) \times \\ &\times \left[\sum_{n=0}^{\infty} (\mathcal{P}_I^O \mathcal{P}_I^O)^n e^{+in(\chi_R - \chi_L)} \right] \times \\ &\times (\Gamma_L e^{-i\chi_L} \mathcal{F}_L^- + \Gamma_R e^{-i\chi_R} \mathcal{F}_R^-). \end{aligned} \quad (\text{D4})$$

After summing the von Neumann operator series we finally obtain Eq. (7).

Similarly, we may recursively construct the trajectories numerically, see Fig. 5. The tunneling during mutually calling control operations is only stopped after no particle tunnels. At infinite bias and infinite feedback strength, the corresponding halting probability vanishes, which leads to a feedback catastrophe. Precursors of this are already observed at finite feedback strength and infinite bias in the large current and Fano factor – compare right columns in tables I and II – or at infinite feedback strength and finite bias in the current – compare the dotted curve in Fig. 2.

Appendix E: Unconditional control leads to transport with the bias

This statement is mainly based on detailed balance, where we assume without loss of generality $f_L < f_R$ at the SET level.

By evaluating the stationary states $\bar{\rho} = (1 - \bar{n}^{\text{SET}}, \bar{n}^{\text{SET}})^T$ of Liouvillians \mathcal{L} , \mathcal{L}_E , and \mathcal{L}_F one can see that their stationary occupation \bar{n}^{SET} is within the transport corridor $f_L \leq \bar{n}^{\text{SET}} \leq f_R$ with the actual position depending on the respective tunneling rates. With any state within the transport corridor as initial condition one can show that the propagators $\mathcal{P} \in$

$\{e^{\mathcal{L}\Delta t}, e^{\mathcal{L}_E\Delta t}, e^{\mathcal{L}_R\Delta t}, e^{\kappa_I}, e^{\kappa_O}\}$ again map to occupations $\rho_{i+1} = (1 - n_{i+1}^{\text{SET}}, n_{i+1}^{\text{SET}})^T = \mathcal{P}(1 - n_i^{\text{SET}}, n_i^{\text{SET}})^T = \mathcal{P}\rho_i$ within the corridor, i.e., for all $f_L \leq n_i^{\text{SET}} \leq f_R$ we have

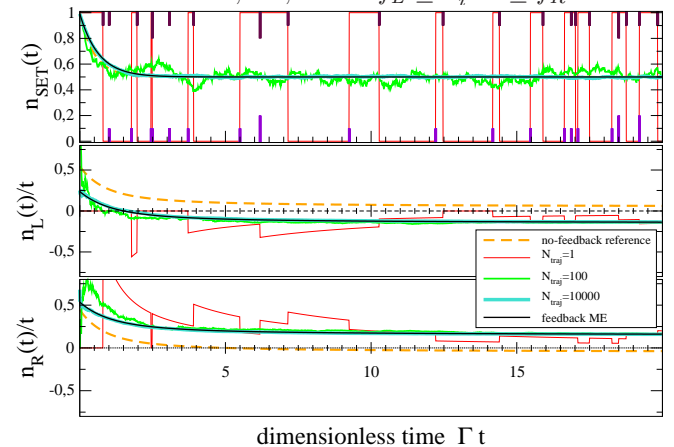


FIG. 5: (Color Online) Comparison of a single (only net changes as in Fig. 4) and the average of 100 and 10000 trajectories with the solution from the effective feedback master equation (7) for the dot occupation (top), the number of particles on the left (middle), and the number of particles on the right (bottom). The average of the trajectories converges to the effective feedback master equation result. Electrons jumping during control operations may now recursively trigger further control operations – marked by the height of the bold kinks in the top graph. Color coding and parameters are as in Fig. 4.

$f_L \leq n_{i+1}^{\text{SET}} \leq f_R$. This implies that once any unconditional iterative control scheme has entered the transport corridor (large times), it will not be able to leave it again, regardless of the timesteps Δt , control parameters, baseline tunneling rates, and the order of the operations. In contrast, with the conditioned feedback scheme one is always outside this corridor with $n_i^{\text{SET}} \in \{0, 1\}$. With inserting counting fields at e.g., the right junction $\mathcal{P} \rightarrow \mathcal{P}(\chi_R)$ one may now calculate the mean particle number tunneling during an iteration step

$$\Delta n_i = (-i) \partial_{\chi_R} \text{Tr} \{ \mathcal{P}(\chi_R) (1 - n_i^{\text{SET}}, n_i^{\text{SET}})^T \} \Big|_{\chi_R \rightarrow 0} \quad (\text{E1})$$

when the initial state is within the transport corridor ($f_L \leq n_i^{\text{SET}} \leq f_R$). The outcome is that in this case the electron current always points from right to left when $f_L < f_R$, i.e., for similar temperatures with the bias.

Note also that for unconditional switching between the Liouvillians (scheme I), this is not a Parrondo game anymore, since a third possibility of game outcome (no tunneling event at all) is included.

Appendix F: Nonlinear Current-Voltage Characteristics

The stationary current (e.g., at the right junction) may either be calculated from the cumulant-generating function or via the relation $I = (-i)\text{Tr} \left\{ \partial_{\chi_R} \mathcal{L}(\chi_L, \chi_R) |_{0,0} \bar{\rho} \right\}$, where $\mathcal{L}(0, 0) \bar{\rho} = \mathbf{0}$ and reads for scheme I

$$I_{\text{fb}}^I = \frac{\Gamma_L \Gamma_R \left[e^{\delta_L^E + \delta_R^E} f_L (1 - f_R) - e^{\delta_L^E + \delta_R^E} (1 - f_L) f_R \right]}{\Gamma_L e^{\delta_L^E} (1 - f_L) + \Gamma_R e^{\delta_R^E} (1 - f_R) + \Gamma_L e^{\delta_L^E} f_L + \Gamma_R e^{\delta_R^E} f_R}, \quad (\text{F1})$$

where insertion of the Fermi functions $f_\alpha = [e^{\beta_\alpha(\epsilon - \mu_\alpha)} + 1]^{-1}$ at similar temperatures $\beta_L = \beta_R = \beta$ and symmetric chemical potentials $\mu_L = +V/2$ and $\mu_R = -V/2$ yields the full nonlinear current-voltage characteristics displayed in Fig. 2. Naturally, the zero-feedback case $\delta_L^E = \delta_R^E = \delta_L^F = \delta_R^F = 0$ reproduces the known results.

For feedback schemes IIa and IIb the expressions become a bit lengthy, such that we only give the maximum feedback limit $\delta_L^I = \delta_R^O = 0$ and $\delta_R^I = \delta_L^O \rightarrow \infty$ for the current

$$\begin{aligned} I_{\text{fb}}^{IIa} &= \frac{f_L(1 - f_R) \left[\Gamma_L^2 (1 - f_L)^2 + \Gamma_R^2 f_R^2 \right] + \Gamma_L \Gamma_R \left[f_L - f_L^2 - f_R^2 - f_L f_R - 2f_L^2 f_R^2 + 2f_L f_R (f_L + f_R) \right]}{\Gamma_L [1 - f_L(1 - f_L + 1 - f_R)] + \Gamma_R [1 - (1 - f_R)(f_L + f_R)]}, \\ I_{\text{fb}}^{IIb} &= \frac{\Gamma_L^2 f_L (1 - f_L) (1 - f_R) + \Gamma_R^2 f_L f_R (1 - f_R) + \Gamma_L \Gamma_R \left[f_L - f_R^2 - f_L^2 f_R + f_L f_R^2 \right]}{\Gamma_L [1 - f_L(1 - f_L + 1 - f_R)] + \Gamma_R [1 - (1 - f_R)(f_L + f_R)]}. \end{aligned} \quad (\text{F2})$$

Again, insertion of the Fermi functions at similar temperatures and symmetric chemical potentials yields the nonlinear current-voltage characteristics in Fig. 2. It also becomes evident that at reverse infinite bias ($f_L \rightarrow 0$ and $f_R \rightarrow 1$), feedback with $\delta_L^I = \delta_R^O = 0$ cannot overcome the large bias voltage, such that the same result as without feedback is obtained. Inserting these highly nonlinear dependencies in the differential equation $\dot{V} = eI(V)/C$ finally yields the inset of Fig. 2.
